arXiv:1212.0930v1 [cond-mat.mes-hall] 5 Dec 2012

$(NH_4)_2S_x$ passivation of the (311)A GaAs surface in AlGaAs/GaAs heterostructures

D.J. Carrad,[1] A.M. Burke,[1] P.J. Reece,[1] R.W. Lyttleton,[1]
D.E.J. Waddington,[1] A. Rai,[2] D. Reuter,[2] A.D. Wieck,[2] and A.P. Micolich[1,*]
[1]*School of Physics, University of New South Wales, Sydney NSW 2052, Australia*
[2]*Angewandte Festkörperphysik, Ruhr-Universität Bochum, D-44780 Bochum, Germany*
(Dated: December 6, 2012)

We have studied the efficacy of $(NH_4)_2S_x$ surface passivation on the (311)A GaAs surface, and in particular, as a possible solution to the gate hysteresis problem in transistors made using Si-doped p-type (311)A AlGaAs/GaAs heterostructures. We report XPS studies of simultaneously-grown (311)A and (100) heterostructures showing that the $(NH_4)_2S_x$ solution removes the surface oxide and sulfidizes both surfaces. Passivation is typically characterized using photoluminescence measurements, and we show that while $(NH_4)_2S_x$ treatment gives a $40-60\times$ increase in photoluminescence intensity for the (100) surface, an increase of only $2-3\times$ is obtained for the (311)A surface. A corresponding lack of reproducible improvement in the gate hysteresis of (311)A heterostructure transistor devices made with the passivation treatment performed immediately prior to gate deposition is also found. We discuss possible reasons for why sulfur passivation is ineffective on the (311)A GaAs surface, and propose several alternative strategies for passivation of this surface.

PACS numbers: 72.25.-b, 73.21.Hb, 85.35.-p

I. INTRODUCTION

Surface effects increasingly influence transport in electronic devices as they are reduced in size. Understanding the influence of the surface, and devising methods for minimizing any detrimental impact on electronic performance is a vital aspect of device development.[1] Semiconductor surfaces are often highly non-ideal, featuring complex surface reconstructions and an abundance of dangling bonds. The latter produce localized energy levels in the surface band structure; these surface states can act as metastable charge trapping sites. The surface states in GaAs pin the surface Fermi energy near the middle of the band-gap causing a high surface recombination rate and difficulties in making ohmic contacts. These present difficulties for GaAs-based devices such as photovoltaic cells and bipolar transistors.[2]

Chalcogenide-based passivation has long been investigated as a route to reducing surface-state problems in III-V semiconductors.[1] A favored route for the passivation of GaAs surfaces is the use of inorganic sulfides such as $(NH_4)_2S$ and Na_2S.[2–7] It involves the removal of the native surface oxide, either as part of the surface sulfidization process itself, or by a separate etch process immediately prior, and binding of S to the Ga and/or As surface atoms. The objective of a passivation treatment is to covalently satisfy all of the Ga and As dangling bonds such that the resulting surface states have energies in either the conduction or valence bands, where they no longer act as charge traps.[1,4,8] This ideal is difficult to achieve, and has resulted in a plethora of passivation chemistries and treatments in both the liquid[3,4,9–13] and gas[14–16] phases. Preceding work has focussed on more basic surface planes such as (100), (110) and (111) due to their applications in device technologies; sulfide passivation of more complex surfaces such as (311)A has not been previously reported. We are interested in (311)A heterostructures as they are an underpinning materials platform for experimental studies of low-dimensional hole systems. Compared to electrons, holes in GaAs have enhanced carrier-carrier interactions due to an increased effective mass and a curious spin-$\frac{3}{2}$ nature caused by strong spin-orbit effects. As a result, there has been much interest in hole systems for studies of novel physics related to the metal-insulator transition,[17,18] bilayer quantum Hall effect,[19,20] Landé g-factor anisotropy,[21–23] anomalous spin-polarization effects,[24] 0.7 plateau in quantum point contacts,[25,26] Berry's phase in Aharonov-Bohm rings[27] and the quantum dot Kondo effect.[28] Hole quantum dots are also of interest for quantum computing applications due to a reduced spin-decoherence time compared to electrons.[29,30]

We present a study of sulfur passivation of the (311)A GaAs surface, motivated by a previous study focussed on understanding the origin of gate hysteresis in field-effect transistor devices made on p-type Si-doped AlGaAs/GaAs heterostructures.[31] Here we use photoluminescence (PL) and x-ray photoelectron spectroscopy (XPS) measurements to analyze the relative efficacy of sulfur treatment on the (311)A and (100) GaAs surfaces. This is combined with electrical measurements of Schottky-gated transistors made using p-type AlGaAs/GaAs heterostructures and different sulfur passivation treatments to determine the corresponding effect on gate stability. We find that sulfur treatment of the (311)A surface removes the native oxide and replaces it with a sulfide layer, as it does for (100), but does not produce a consistent, corresponding improvement in photoluminescence intensity or gate stability for transistors. We discuss possible reasons for this lack of efficacy in electronic passivation and offer some potential strategies for improved passivation for the (311)A surface. We also briefly discuss some of the practical issues that we faced in translating the sulfur treatments we studied, which are normally used on bare semiconductor surfaces, to the polymer resist based fabrication typical for transistor devices.

II. METHODS

A range of possible sulfur treatment formulations exist, including: using aqueous solutions of Na_2S, $(NH_4)_2S$ or Li_2S,[3,4], alcoholic solutions of Na_2S[9] and $(NH_4)_2S$,[10,11] S_2Cl_2 in CCl_4,[11,12] electrochemical growth of a sulfur-containing anodic oxide film,[13] exposure to H_2S gas[14,15] or UV photosulfidation using a molecular sulfur vapor.[16] We focussed on Na_2S and $(NH_4)_2S$ based solutions as they provide the best mix of ease and effectiveness. While Na_2S is reported to produce a surface passivation that is more robust to light/oxygen than $(NH_4)_2S$ treatment,[32] treatment with $(NH_4)_2S$ gives complete oxide removal, and produces a more sulfidized surface with no traces of Na.[7,33] This behavior can be enhanced by adding elemental sulfur i.e., treating with $(NH_4)_2S_x$.[34,35] As a result, aqueous $(NH_4)_2S$ and $(NH_4)_2S_x$ solutions are commonly used for passivation of structures ranging from GaAs metal-insulator-semiconductor field-effect transistors (MISFETs)[36] to InAs/GaSb photodiodes[37] to III-V nanowire devices.[38] Hence, for the vast majority of this study we restrict ourselves to aqueous $(NH_4)_2S_x$ solutions. The exception is the study of passivation solution compatibility with the polymer resists used for photolithography (MicroChem S1813/AZ nLOF2020) and electron-beam lithography (MicroChem 950k-A5 polymethylmethacrylate) reported in Appendix A. Here we tested aqueous and alcoholic solutions of Na_2S and $(NH_4)_2S$ applied immediately prior to photodefined gate deposition. The only compatible treatment was aqueous $(NH_4)_2S$ and $(NH_4)_2S_x$, further supporting our choice to study the passivation efficacy of this treatment alone.

Two different concentrations of aqueous $(NH_4)_2S_x$ solution were investigated, denoted as 'weak' and 'strong'. Both were made from a common stock solution prepared by adding 3 mol/L of elemental sulfur (Aldrich) to 20% $(NH_4)_2S$ in H_2O (Aldrich) decanted as supplied. The stock solution is stirred for several hours until the sulfur is completely dissolved, and then stored in a brown glass bottle inside a closed metal can to prevent photodecomposition. The strong treatment involves immersion of the sample in decanted stock solution for 10 min, while the weak treatment involves immersion in a 0.5% dilution of stock solution in deionized water for only 2 min. In both cases, treatment involves immersion in $3 - 5$ mL of passivation solution heated to 40°C in a water bath.[36] Prior to passivation, all samples were given a 30 s deoxidizing etch in 31% HCl:H_2O. After passivation they are rinsed in deionized water and dried with N_2 gas. Prolonged exposure to light and air can result in surface reoxidation;[39] hence devices were stored in the dark between passivation and any subsequent fabrication steps or measurements.

Commenting briefly on relative passivation solution strength, the weak treatment was more dilute than commonly used solutions. Treatment times of $10 - 15$ mins with $(NH_4)_2S_x$ concentrations of $5 - 20\%$ are typically quoted in the literature.[40–43] However, the effectiveness of the weak solution has been previously established for passivating InAs nanowires.[38] In Ref.[38] the nanowires were etched, sometimes completely through, consistent with the etching of GaAs found in Ref.[35]. We focused on the weak treatment here because the heterostructures used for the devices have only a thin GaAs cap layer protecting the active AlGaAs and GaAs layers underneath and we wanted to avoid the risk of exposing the AlGaAs, which would oxidize rapidly in air, or generating significant surface roughness due to etching by the $(NH_4)_2S_x$ treatment. We also tested the strong treatment on our devices to check that insufficient treatment solution concentration was not responsible for the lack of efficacy in passivation (see Section III-C).

Two types of GaAs substrates were used: epitaxially-grown AlGaAs/GaAs heterostructures modulation-doped with Si were used for device fabrication and XPS studies, while 'bulk' GaAs substrates without any epilayers were used for the PL studies. We used bulk wafer in the latter instance because the heterostructure epilayers interfered with the surface PL signal. A set of matched (100)/(311)A AlGaAs/GaAs heterostructures (Bochum 13473/13516) were custom grown side-by-side using molecular beam epitaxy for this experiment. They have a nominally identical epilayer structure, with the active region consisting of 650 nm undoped GaAs, 35 nm undoped $Al_{0.34}Ga_{0.66}As$, 80 nm Si-doped $Al_{0.34}Ga_{0.66}As$ and a 5 nm undoped GaAs cap. These matched heterostructures have majority carriers of opposite sign – n-type for (100) and p-type for (311)A – due to the amphoteric nature of Si dopants in AlGaAs.[44]

For all samples, semiconductor pieces approximately 3×4 mm^2 were cleaved from the host wafer and thoroughly cleaned with acetone and 2-propanol. Samples prepared for XPS/PL measurements then underwent sulfur passivation as described above, with the samples typically measured within 30 min of passivation to avoid re-oxidation of the surface.

For device-related studies, photoresist was deposited onto the cleaned wafer piece using a standard resist-spinning technique. Hall bars with a height of 130 nm were defined by photolithography and wet etching using a $2:1:20$ buffered HF:H_2O_2:H_2O solution (the buffered HF was 7:1 NH_4F:HF). Ohmic contacts for the (311)A heterostructure pieces were formed by vacuum evaporation of a 150 nm thick 99:1 Au:Be alloy film, which was annealed at 490°C for 90 s. Electrical studies of the (100) heterostructures were presented in Ref.[31]. The Schottky gates were defined photolithographically using AZ nLOF2020 photoresist, with development in 2.38% tetramethylammonium hydroxide (TMAH) solution. Sulfur passivation was performed after development, and immediately before vacuum deposition of the gate metal, consisting of a 20 nm Ti adhesion layer fol-

TABLE I. List of samples discussed in this paper. Bulk GaAs wafer pieces used for PL are labeled B1 - B4. Unpassivated reference pieces used in the PL studies have been excluded from the data for simplicity. Heterostructures without devices used for XPS studies are labeled H1 - H4. Modulation-doped heterostructure devices used for gate hysteresis studies are labeled D1 - D6.

Sample	Wafer	Surface	Passivation
B1	bulk	(100)	strong
B2	bulk	(100)	weak
B3	bulk	(311)A	strong
B4	bulk	(311)A	weak
H1	13516a	(100)	none
H2	13516a	(100)	weak
H3	13516b	(311)A	none
H4	13516b	(311)A	weak
D1	13516b	(311)A	none
D2	13473b	(311)A	weak
D3	13516b	(311)A	weak
D4	13473b	(311)A	weak
D5	13516b	(311)A	strong
D6	13516b	(311)A	strong + anneal

lowed by a 80 nm Au layer. The passivated samples were stored in deionized water (18 MΩcm) during transfer to the metal evaporator, and exposed to air for at most a few minutes before the evaporator chamber containing the sample reached vacuum (< 1 mTorr). Such short exposures to air should not lead to significant surface reoxidation,[39] as confirmed by our PL data in Appendix B. The devices were completed by lift-off in acetone and bonding into chip packages using an Au ball bonder. After metal deposition we expect the passivated surface to remain robust to reoxidation since it is protected from light and air by the gate metal.[39] Table 1 lists the samples/devices studied along with the wafer type, surface orientation and passivation treatment used.

The effect of $(NH_4)_2S_x$ passivation on the surface chemical composition and surface-state density was determined using room temperature PL and XPS measurements. Photoluminescence (PL) measurements were performed under ambient conditions to characterize the effect of surface passivation. Samples were excited using the 488 nm line of an argon ion laser (Coherent Innova 70) and the luminescence was coupled to a 0.27m grating spectrometer (J/Y SPEX 270M) and recorded with a charge-coupled device (Princeton Instruments). The spectral resolution of the system was 3 nm. The incident power was 1 mW and the intensity at the focus was approximately 0.49 $\mathrm{W.mm^{-2}}$. PL spectra presented here are normalized to the peak intensity of a corresponding unpassivated reference sample. XPS measurements were performed using a ThermoScientific ESCALAB250Xi system with a monochromated Al Kα source ($h\nu = 1486.68$ eV at 164 W power). A spot size of 500 μm was used with a photoelectron take-off angle of 90°. The C(1s) peak at 285.0 eV is used as the binding energy reference for all measurements performed; the measured binding energies are expected to be accurate to ±0.1 eV. The XPS data peak fitting was performed using the Avantage software package.

Electrical studies of passivated/unpassivated devices made on modulation-doped heterostructure were performed with standard four-terminal ac lock-in techniques at $T = 4.2$ K. The drain current I_d was measured with an applied source-drain bias $V_{sd} = 100\ \mu$V at a frequency $f = 73$ Hz. A dc gate bias V_g was applied using a Keithley 2400 source-measure unit with a built-in adjustable current limiter to prevent the gate being driven to biases where the gate leakage current I_g becomes excessive.

III. RESULTS

A. XPS study of the effect of $(NH_4)_2S_x$ on the (311)A GaAs surface

We now discuss our XPS studies of bare and passivated (311)A GaAs surfaces. The surface sulfidization chemistry for bare and passivated (100) GaAs surfaces is well characterized using XPS.[6,7,32,45–49] In this study, bare and passivated (100) surfaces were prepared and measured in parallel for reference to provide more direct, like-for-like comparison, and to better isolate the effect of surface orientation on the passivation chemistry. XPS data for passivated and unpassivated samples is presented in Fig. 1(a/c/e) and (b/d/f) for the (100) and (311)A surfaces, respectively. We begin with the As($2p_{3/2}$) core level spectra in Fig. 1(a/b), where the unpassivated surfaces show peaks corresponding to GaAs (1323.2 eV) and As_2O_3 (1326.3 eV) for both surface orientations. After passivation, the As_2O_3 peak is eliminated and a small peak (1324.5 eV) corresponding to the disulfide bridges reported by Sandroff *et al.*[32] for $(NH_4)_2S$ passivation of (100) GaAs is observed; this peak emerges to a roughly equivalent extent for both the (100) and (311)A surfaces in our study. We now turn to the Ga($2p_{3/2}$) spectra in Fig. 1(c/d). The unpassivated surfaces in both cases show peaks corresponding to GaAs (1117.4 eV) and Ga_2O_3 (1118.5 eV). The Ga_2O_3 peak intensity for the (100) surface, relative to the GaAs peak, is roughly double that for (311)A. This likely reflects the fact that surface Ga atoms have single dangling bonds for (311)A but double dangling bonds for (100).[53,54] Looking at the passivated samples, there is a clear Ga peak and a weaker peak at higher energy, which may correspond to Ga-S bonding but could also be due to residual Ga_2O_3; unfortunately, the low peak intensity makes conclusively assigning the source difficult.

Instead we turn to the combined Ga(3s)/S(2p)spectra in Fig. 1(e/f). Here the unpassivated surface gives a pair of peaks at 156.4 and 160.4 eV corresponding to GaAs bonds, with the passivated samples displaying the addition of small peaks at 163.3 and 162.1 eV. The most likely attribution for these peaks is that they correspond to As-S and Ga-S bonds (expected at 163.2 and 162.3 eV)

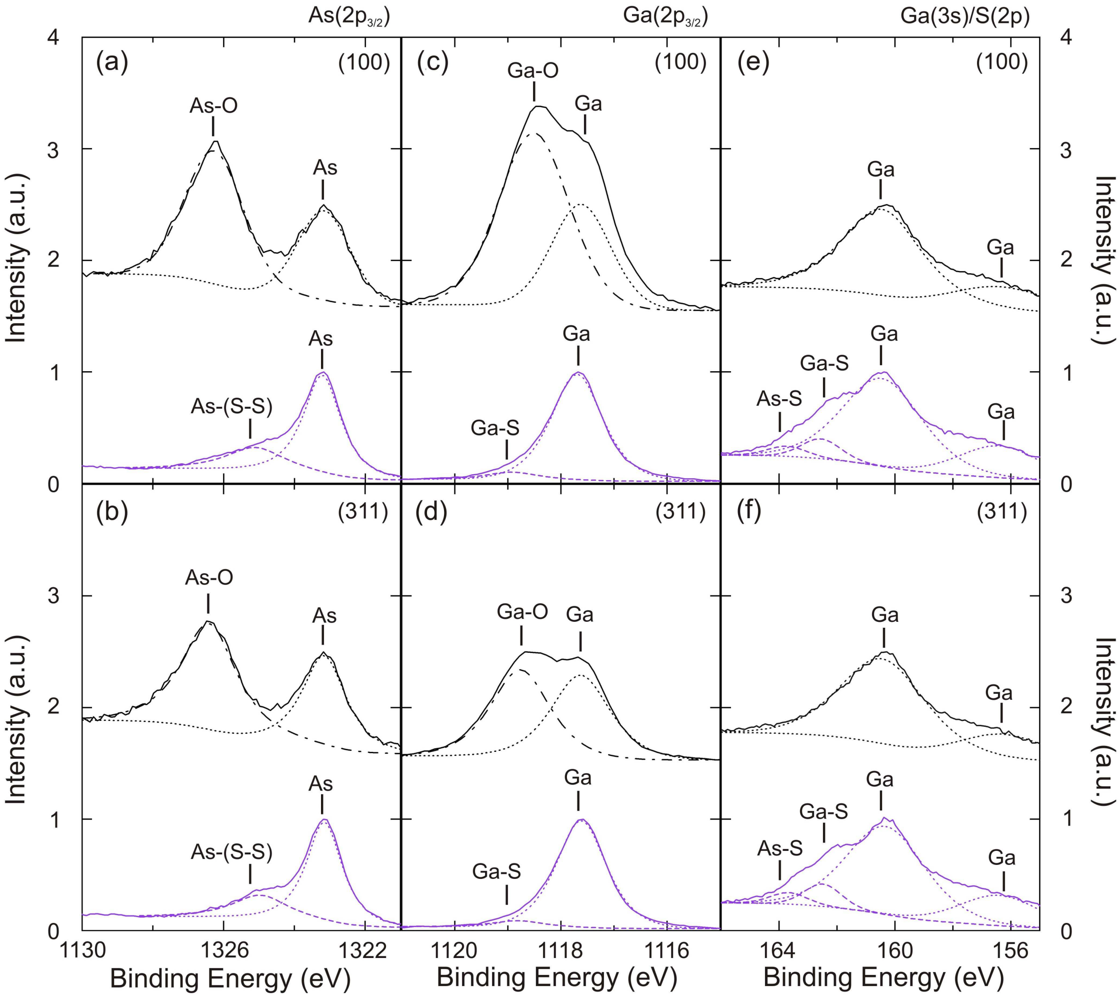

FIG. 1. (Color online) (a,b) As($2p_{3/2}$), (c,d) Ga($2p_{3/2}$) and (e,f) Ga(3s)/S(2p) XPS core level spectra for passivated (purple/lower traces) and unpassivated (black/upper traces) GaAs surfaces with (100) (top row) and (311)A (bottom row) orientation. In each case the intensity is normalized to the Ga-As peak, with the unpassivated intensities offset vertically by 1.5 for clarity. Solid lines are the measured spectra, the dotted and dashed lines are peak fits for the Ga-As and X-Y spectral peaks, where X = Ga,As and Y = S,O, respectively. The data shows that passivation treatment removes the surface oxide, replacing it with a surface sulfide layer (c.f. Refs.[32,51]).

respectively, as reported for (100) GaAs surfaces passivated with $P_2S_5/(NH_4)_2S_x$ solution.[51] However, we note an alternate possibility that one or other of these peaks corresponds to a disulfide bridge (expected at 163.5 eV), as reported for $(NH_4)_2S_x$ passivated (100) InGaP surfaces.[50] Ultimately, the strong similarities between the XPS spectra suggest that the passivation treatment removes the surface oxide and establishes a surface sulfide layer for both surfaces with roughly equivalent efficacy.

B. Comparative photoluminescence study of $(NH_4)_2S_x$ treated (100) and (311)A GaAs surfaces

Remarkably, a corresponding equivalency was not observed in photoluminescence measurements of passivated surfaces for the two different orientations. Figure 2 shows PL spectra for (a) the (100) and (b) the (311)A surfaces after passivation with the strong (solid line) and weak (dashed line) $(NH_4)_2S_x$ solutions. In each case, the intensity is normalized to the peak intensity of the PL spectra for an unpassivated surface with matching orientation (see Appendix C). In other words, a given passivated sample's peak PL intensity, as presented in our data, represents the factor by which passivation increases the PL due to reduced surface recombination velocity.[4,52] Figure 2 shows that the passivation has increased the PL intensity of (100) GaAs by $40 - 65\times$, but only increased the PL intensity of (311)A GaAs by $2 - 3\times$. This approximately 20× difference suggests that the passivation is much less effective on (311)A GaAs than it is on (100) GaAs. This difference is likely to arise from Ga rather than As because unlike As, which presents a double-dangling bond on both surfaces, sur-

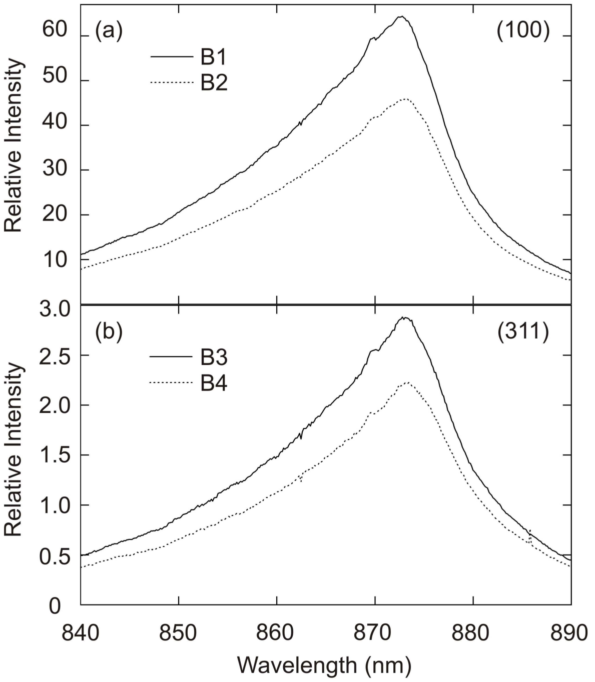

FIG. 2. Photoluminescence intensity vs wavelength for (a) Samples B1 and B2 with (100) surfaces passivated with strong (solid line) and weak (dotted line) solution, respectively, and (b) Samples B3 and B4 with (311)A surfaces passivated with strong (solid line) and weak (dotted line) solution, respectively. The PL intensity in both cases is normalized to the PL spectra obtained for an untreated sample with the same surface orientation. The approximately 20× difference in PL intensity may be due to the difference in Ga dangling bond valence between the (100) and (311)A surfaces[53,54].

face Ga presents a double-dangling bond for (100) and a single-dangling bond for (311)A.[53,54] Although there is no corresponding difference in Ga-S and As-S XPS peaks between (100) and (311)A in Fig. 1, the different Ga dangling bond valence for (311)A may mean that sulfur atoms are unable to bond to Ga surface such that all dangling bonds are satisfied. This could result in a higher surface-state density for the passivated (311)A surface compared to (100), explaining the lowered PL intensity observed for the (311)A surface in Fig. 2(b). We will discuss this further in Section IV.

C. Effect of passivation on gate hysteresis in (311)A heterostructure devices

Gated Hall bars made using Si-doped (311)A AlGaAs/GaAs heterostructures display strong gate hysteresis with an anticlockwise hysteresis loop in the I_d versus V_g characteristics. This hysteresis is consistent with trapping of net negative charge between the gate and the 2DHG, either in surface-states or the modulation doping layer.[31] An example of a typical hysteresis loop obtained from an unpassivated (311)A device is shown in Fig. 3(a). The most striking feature is the long plateau at intermediate V_g whilst sweeping the gate to positive bias. Here, depletion of the 2DHG is strongly suppressed due to charge trapping in the surface-states and/or charge migration in the dopant layer. Depletion resumes for sufficiently positive V_g, and in most Schottky-gated devices we have studied, pinch-off (i.e., $I_d = 0$) can be attained before V_g exceeds +1 V. The length the current plateau and the pinch-off voltage provide a measure of charge trapping/migration within the device. Hence a reduction in surface-state density, due to passivation for example, should result in a reduced I_d plateau length and a lower pinch-off voltage.

Figures 3(b-f) show the electrical characteristics that result for devices D2-D6 made with different sulfur passivation treatments prior to gate deposition. The results obtained with the weak passivation solution vary, with the current plateau extending (Fig. 3(b)), shortening (Fig. 3(c)), and in an isolated instance, disappearing entirely (Fig. 3(d)). The behavior observed in Fig. 3(b/c) is most typical; across the five devices we studied using the weak passivation treatment we observe pinch-off voltages ranging from +0.25 V to +0.8 V and plateau lengths ranging from 0 V to +4.75 V. We have not been able to reproduce the outcome for device D4 (Fig. 3(d)) in a second, separate device despite numerous attempts; yet the characteristics we report here were repeatable for subsequent cooldowns of the same device (i.e., the treatment was robust). With a more focussed surface chemistry study it may be possible to identify a method for reliably producing an outcome similar to that in device D4.

A possible argument for the inconsistent results obtained in Figs. 3(b-d) is that the passivation treatment is not strong enough. In Fig. 3(e) we show the results of an attempt to more effectively passivate the GaAs surface. Device D5 was prepared using the 200× more concentrated passivation solution, and although the current plateau at intermediate V_g is weakened (i.e., appears less as a constant I_d plateau and as more a region of reduced depletion rate), there is little reduction in pinch-off bias and the device becomes more unstable/erratic at low I_d. This may suggest that the inefficacy of passivation treatment on the hysteresis is not related to insufficient sulfidization.

Post-passivation annealing is an informative experimental tool because the large difference in Ga-S and As-S bond stability[33,55] means that annealing increases Ga-S bonding at the expense of As-S bonding by breaking As-S surface bonds, transferring S to Ga, and at sufficiently high temperatures, desorbing excess As.[33,45,46,56,57] Little is known about the sulfur chemistry of the (311)A surface, but since (311)A surface As atoms are (100)-like (see Section IV), we assume here that desorption of As surface bonds is complete for samples annealed above 350°C, as found for the (100) GaAs surface.[47,57,58] To determine the influence that As-S bonds have on the electrical characteristics, device D6 was prepared using

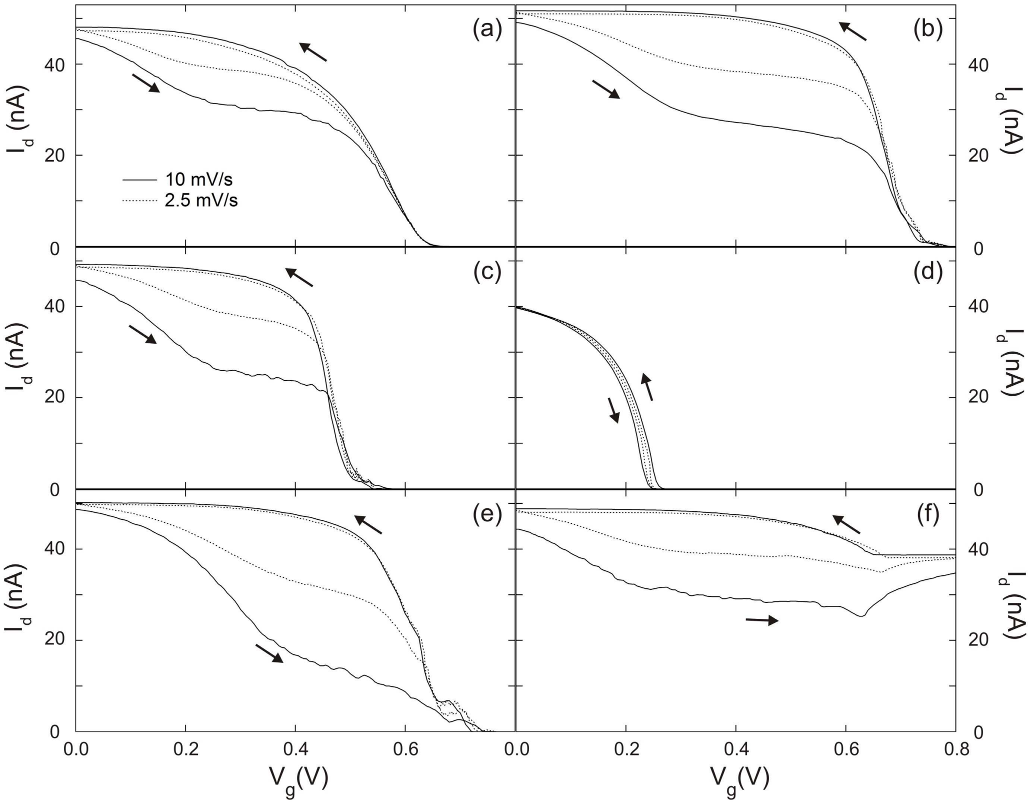

FIG. 3. Drain current I_d vs gate bias V_g characteristics for Devices (a) D1 - unpassivated, (b-d) D2-D4 - weak passivation, (e) D5 - strong passivation and (f) D6 - strong passivation and a post-passivation anneal at 360°C for 10 min in an Ar atmosphere. The arrows indicate the sweep direction (upsweep/downsweep) for the two components of each hysteresis loop; the solid (dashed) lines are data for V_g sweep rates of 10(2.5) mV/s, respectively. Pinch-off could not be achieved for Device D6; the gate begins to leak strongly as V_g approaches +0.6 V. The rise in I_d for positive $V_g > +0.61$ V (upsweep), and corresponding plateau in I_d in the return to $V_g = +0.61$ V (downsweep) occur due to the current limiting action of the gate voltage source, which effectively holds $V_g = +0.61$ V for $V_g > +0.61$ V where $I_g > 50$ nA.

the strong solution followed by a post-passivation anneal for 10 min at 360°C. The sample was held at a 1 atm Ar atmosphere for the entire anneal process including warm-up from and cool-down back to room temperature to prevent oxidation. Photoprocessing and metallization was performed as soon as possible thereafter, with extra care taken to keep the sample away from light to avoid photo-oxidation. The robustness of passivation to subsequent photo-processing is discussed in Appendix B.

Post-passivation annealing appears to be detrimental for the (311)A surface; as Fig. 3(f) shows, pinch-off cannot be achieved in these devices. The current plateau on sweeping to positive V_g begins at a lower V_g and extends such that gate leakage exceeds the limit set by the gate voltage source before the end of the current plateau (c.f. Fig. 2 of Ref.[31]). The lack of carrier depletion in Fig. 3(f), particularly at low V_g, suggests that As surface states play an important role in the hysteresis. The corollary is that As-S bonding is beneficial to reduced hysteresis, which would explain why it was possible to achieve hysteresis-free behavior in device D4. The variability in passivation efficacy that we find in Figs. 3(b)-(d) may also be a symptom of the low As-S bond stability,[33,55] which leads to surface As accumulation and As-As and As-O surface bond formation with H_2O washing.[48,58,59] This would make aqueous passivation treatments a considerably more capricious and variable prospect. Ultimately, gaseous treatments may be more viable for passivation of the (311)A surface as they avoid both water, and the organic solvents that are incompatible with conventional device fabrication processes (see Appendix A).

We also found that gates on (311)A surfaces that underwent post-passivation annealing tend to be more leakage prone. One possible explanation for the leakage prone gates is Be diffusion from the ohmic contacts; the contacts are deposited and annealed prior to the passivation and post-passivation anneal. Although the post-passivation anneal is 130°C lower in temperature than the ohmic contact anneal, its duration is more than six times longer. The rapid diffusion and surface aggregation of Be in GaAs is well known.[60]

Returning briefly to device D4 where the hysteresis is almost eliminated, it is tempting to think that the surface-state density within the band-gap has been dramatically reduced for this device. However, the same behavior could be expected if there was a sharp reduction in the tail of the surface-state spectrum or if the spectrum changed such that a large density of surface-states was energetically shifted away from the surface Fermi energy. In both instances, reduced charge trapping at low gate bias would result in rapid depletion, allowing the device to reach pinch-off before onset of the current plateau. It may only take a partially effective passivation to achieve this, and device D4, although a one-off example, indicates that a surface passivation treatment able to significantly reduce the gate hysteresis observed in (311)A heterostructure devices may exist.

IV. DISCUSSION

Drawing together the XPS, PL and electrical measurements presented above, it is evident that $(NH_4)_2S_x$ treatment removes oxide and sulfidizes the surface for both orientations. The enhancement in PL intensity is smaller for the (311)A surface, and correspondingly, there is little improvement in the gate hysteresis for p-type modulation-doped (311)A AlGaAs/GaAs heterostructure devices. We came into this study expecting, perhaps naïvely, that sulfur passivation may mitigate the gate hysteresis;[31] instead we are left with several questions: Why is it that the $(NH_4)_2S_x$ treatment produces a clear chemical change in the (311)A surface with little corresponding improvement in electrical properties? Is there something about the nature of the (311)A GaAs surface that would make this an expected behavior? Is there some insight for how a more effective passivation treatment might be formulated? In this final section, we attempt to answer these questions.

Higher Miller-index surfaces tend to present as linear combinations of lower Miller-index surfaces. In particular, the (311) surface can be roughly considered as the average of the (100) and (111) surfaces, with equal densities of (111)-like single-dangling and (100)-like double-dangling bond sites.[44,61] Additionally, unlike ideal (100) and (111) surfaces, where the surface dangling bonds are nominally all of the same molecular species (i.e., either Ga or As), the ideal (311) surface presents dangling bonds for both molecular species in equal proportions. The (311)A surface studied here presents (100)-like As double-dangling bonds and (111)-like Ga single-dangling bonds to the vacuum, nominally with a (1×1) surface reconstruction,[54] although the (311)A surface is suggested to show numerous metastable reconstructions.[62] We propose that the bimolecular nature of the (311)A surface is central to the observed inefficacy of sulfur passivation despite the clear sulfur binding signature in the XPS data (Fig. 1). For clarity of later discussion, we will first briefly review how $(NH_4)_2S_x$ treatment affects the surface Ga and As atoms on (100) and (111)A GaAs surfaces.

The initial $(NH_4)_2S_x$ treatment leads to a surface containing Ga-S, As-S and surface-bound S-S dimers; however because the As-S bond is thermodynamically much less stable than the Ga-S bond,[33,55] rinsing with water leaves Ga-S bonds in the majority with the remaining surface-bound S forms (e.g., As-S, As-(S-S), etc.) washed away.[48,59] Thermal annealing exacerbates this trend towards the dominance of Ga-S bonds.[33,45,46] The dominance and robustness of Ga-S bond makes it the logical first consideration. For the (100) surface, the Ga-bound S atom adopts a Ga-S-Ga bridge configuration[63,64] to satisfy the double-dangling bond of the bare surface Ga. Total energy calculations based on a density-functional formalism suggest this gives Ga-S bonds with bonding and anti-bonding orbitals that sit within the valence and conduction bands, respectively (i.e., outside the band-gap).[65] When combined with a possible tendency for the sulfur treatment to preferentially generate Ga-terminated surfaces in the (100) orientation,[33] and the high Ga-S bond stability, this should result in a substantial and robust reduction in the Ga-related mid-gap surface-state density for (100) GaAs, and a depinning of the surface Fermi level. Indeed, a substantial reduction in Ga-related surface state density close to the conduction band has been observed in capacitance-voltage (CV) and deep level transient spectroscopy (DLTS) measurements of passivated (100) GaAs surfaces.[2,34,36] For the (111)A surface, the Ga-bound S atom sits on top of the surface Ga atom to satisfy the single-dangling bond of the bare surface Ga.[66–68] Calculations suggest that the bonding and anti-bonding orbitals sit inside the band-gap in this case.[69] Hence Ga-related mid-gap states on the unpassivated (111)A surface are replaced by Ga-S states closer to the valence band for a passivated (111)A surface, which should lead to the surface Fermi energy pinning closer to the valence band maximum rather than depinning completely.[69] That said, experiments suggest that the surface Fermi energy moves away from the valence band maximum upon passivation of the (111)A surface,[68] possibly as a result of S replacing some uppermost sub-surface As atoms in addition to bonding to surface Ga. Either way, the efficacy of sulfur passivation for the (111)A surface would be diminished compared to the (100) surface.[68]

The behaviour of surface As is a more difficult prospect because although surface As for the (311)A surface is (100)-like and passivation of the (100) GaAs has been heavily studied, the role of As-S bonding in passivation of (100) GaAs is still poorly understood. For example, some theoretical studies suggest that the As-S anti-bonding state for (100) GaAs sits well within the band-gap[65,69], while other calculations place these states within the valence band.[70] On the experimental side, there is much debate about the role and importance of As-S bonding also. Some studies point to As-S and As-(S-S) being central to passivation;[7,47,71] others suggest that the Ga-S bonds are key,[48,57,58] and some argue for the direct involvement of both Ga-S and As-S bonds.[72] Part of the difficulty here is the relative weakness of the As-S bond and the tendency for As accumulation at the surface, which brings about additional mid-gap levels.[58]

Returning now to consider (311)A specifically, while the (100) surface is essentially a best case scenario, the (311)A surface is essentially a worst case scenario. First, the Ga dangling bonds are (111)-like such that Ga-S bonding is likely to produce states within the bandgap.[61,69] Second, the surface should display equal proportions of Ga and As dangling bonds,[44,61] unlike (100) and (111), which could in the ideal case be terminated entirely with Ga dangling bonds. This means that surface As will always be an issue, and our data in Fig. 3 appears to confirm the importance of surface As bonding for the (311)A surface. It also means that (311)A surface passivation will always be difficult, compromised by the relative weakness of the As-S bond to H_2O exposure in particular.[48,58,59] Finally, as mentioned earlier, the (311)A surface can display metastable reconstructions,[62] which may further complicate the surface chemistry and electronic states. We note at this point that this explanation for inefficacy of sulfur passivation for the (311)A surface is simplistic; theoretical studies similar to those in Refs.[65,69] and surface studies similar to those in Refs.[47,68] would significantly enhance understanding. Studies of the (311)A GaAs surface-state spectrum using either capacitance-voltage measurements[34,72,73] or deep-level transient spectroscopy measurements[2] would also be valuable.

This leaves the final question of whether there is a formulation that might passivate the (311)A GaAs surface more effectively. The problem here is twofold, as both the Ga and As surface atoms need attention. The problem with Ga for the (311)A surface is that it has a monovalent dangling bond and sulfur is divalent. An alternative would be a monovalent adsorbate such as chlorine; Cl passivation of GaAs (111)A surfaces by treatment with HCl has been demonstrated.[74] We find that HCl treatment for (311)A heterostructure devices brings no tangible improvement in gate hysteresis (HCl is commonly used as a deoxidation etch prior to gate deposition), however, recent studies have shown that post-chloridation thermal annealing, possibly combined with hydrazine treatment, can significantly enhance Cl passivation efficacy by removing excess As[75]. Further studies of more complex Cl treatments for the (311)A GaAs surface would be of interest. Turning now to As, which is (100)-like for the (311)A surface, an obvious alternative to consider is Selenium. There are several reports of Se treatments being more effective than sulfur treatment and having improved stability against oxidation.[76,77] The greater subsurface penetration of Se[49,78,79] may also be favorable assuming an As antisite defect model[80] for GaAs surface states. It would be of interest to study the effect of Na_2Se in NH_4OH followed by $Na_2S_{(aq)}$,[76] or SeS_2 in CS_2,[77] on the (311)A surface, but an alternative that should also be considered is Se-loaded $(NH_4)_2S$.[81] Note that this would only deal with surface As, passivation of the (111)-like surface Ga bonds would entail additional treatment.

Ultimately, As-chalcogen bond stability and surface As accumulation may still be an issue even with Se-passivation, and a better alternative might be to address this problem by engineering the capping layer of the heterostructure rather than relying on chemical surface passivation treatments. Two possibilities are immediately apparent. The first is to grow a thin cap layer of GaS, which would bury the GaAs surface and perhaps provide better chemical stability for the As most proximal to the surface, while at the same time providing the Ga-S surface bonds shown to be desirable in sulfur passivation treatments. Studies of GaS-capped GaAs have shown promise for this approach on the (100) and (111)A surfaces.[82–84] The one possible issue with this approach would be the compatability of GaS with the ultra-clean molecular-beam epitaxy systems used to grow the high mobility AlGaAs/GaAs heterostructures used for quantum device research. The second, as proposed in Ref.[31], is to grow a degenerately-doped GaAs cap layer, which can be partitioned by wet-etching to form gates for the device, as in undoped Heterostructure Insulated Gate Field Effect Transistors (HIGFETs)[85–87]. The advantage here is that the conducting channel is screened from the surface-states by the highly-conductive cap layer/gate, the disadvantage is that device processing is more complex in such structures.

V. CONCLUSIONS

We have studied the efficacy of $(NH_4)_2S_x$ treatment for surface-state passivation in (311)A AlGaAs/GaAs heterostructures, as a prospective solution to the gate hysteresis problem in nanoscale devices made using this material. We first performed XPS studies on (311)A and (100) heterostructures grown simultaneously by molecular beam epitaxy. These show that the chemistry is very similar for both surface orientations, with the $(NH_4)_2S_x$ solution stripping surface oxides and sulfidizing the surface. Photoluminescence measurements for the two surface orientations showed an improvement in PL intensity by a factor of 40-65 and 2-3 for the (100) and (311)A surfaces, respectively, relative to untreated surfaces after sulfur passivation treatment. The comparative lack of efficacy of sulfur passivation for the (311)A surface evident in PL measurements is consistent with a lack of reproducible improvement in the gate hysteresis of heterostructure transistor devices made with the passivation treatment performed immediately prior to gate deposition. We suggest that the lack of passivation for the (311)A surface, despite an obvious change in the surface chemistry, comes about due to the mixture of monovalent Ga and divalent As dangling bonds it presents to the vacuum. Further work on the passivation of the (311)A surface is encouraged and would include Cl- or Se-based treatments or the addition of a GaS or degenerately-doped GaAs cap layer as alternative strategies for passivation of this surface.

ACKNOWLEDGMENTS

This work was funded by Australian Research Council Grants DP0877208, FT0990285 and FT110100072. DR and ADW acknowledge support from DFT SPP1285 and BMBF QuaHL-Rep 01BQ1035. This work was performed in part using the NSW node of the Australian National Fabrication Facility (ANFF) and the Mark Wainwright Analytical Center at UNSW. We thank Dr Bill Bin Gong for performing the XPS measurements reported here, Tim Bray for assistance with some PL measurements and useful discussions, and Oleh Klochan and Alex Hamilton for helpful discussions.

Appendix A: Practicality of incorporating $(NH_4)_2S_x$ passivation into device processing

To incorporate sulfur passivation into device processing, it was essential that the passivation treatment left the photoresist intact such that we could deposit a photolithographically-defined, shaped gate such as that in Fig. 4(a) and (c). Hence we began with a study of the photoresist compatibility of the various sulfur passivation solutions that we initially intended to use; these included Na_2S and $(NH_4)_2S$ solutions with 2-propanol, 2-methyl-2-propanol (t-butanol) and water as the dilutant for the stock solution. The study was conducted with 3 × 4 mm pieces of the bulk, epilayer-free wafer coated with three different types of resist: MicroChem S1813, a positive photoresist; AZ nLOF2020, a negative photoresist; and MicroChem 950k molecular weight polymethylmethacrylate (PMMA), a positive electron-beam lithography (EBL) resist.

Considering the alcoholic solutions first, while alcoholic passivation is more effective,[39] photoresist tends to be soluble in alcohol. Immersing patterned photoresist in a 2% solution of $(NH_4)_2S_x$ stock solution in 2-propanol began to smear out the pattern within a few seconds. The photoresist was completely removed if the sample was immersed for longer than 15 s, a period insufficient for effective passivation of the exposed GaAs surface. Similar results were obtained in 2-methyl-2-propanol; an example where gate deposition was attempted after $(NH_4)_2S_x$ passivation in a 2-methyl-2-propanol solution is shown in Fig. 4(b). Clearly the gate has not been properly formed; the gate metal covers large regions of the surface where the photoresist was unintentionally removed by the passivation solution. The results for PMMA were more favorable. PMMA has a low solubility in 2-propanol, and films remained intact for immersions in $(NH_4)_2S_x$/2-propanol solutions for as long as 15 min. This is sufficient for effective passivation of patterned areas, but the electron-beam lithography requirement is impractical for large area devices. Qualitatively similar results were obtained for Na_2S solutions in 2-propanol and 2-methyl-2-propanol.

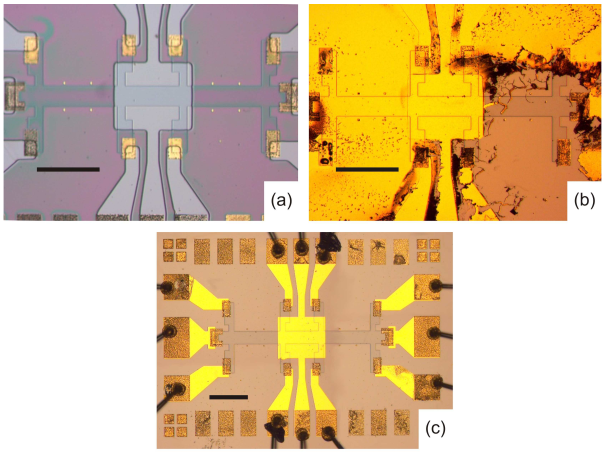

FIG. 4. (Color online) Optical micrographs of (a) a device immediately before passivation and gate deposition, (b) a device after gate deposition that had been passivated with a 2-methyl-2-propanol solution and (c) a completed device. The outline in the middle of the device is the 130 nm high hall bar mesa, the grainy gold regions are the annealed AuBe ohmic contacts and the bright yellow regions are the Ti/Au gates and leads. In (a), the purple region is the resist that has been developed into the negative of the gate pattern. In (b), the gate metal is poorly defined and covers a large area of the device due to the photoresist being dissolved in the alcohol passivation solution. The black scale bars in all images represent 300 μm.

Turning now to aqueous solutions, we found a marked difference between Na_2S and $(NH_4)_2S_x$ based solutions for photoresist films. Photoresist films remained intact for at least 10 minutes for $(NH_4)_2S_x$ based solutions whereas there was significant resist damage for even quite short immersions in Na_2S based solutions ($\lesssim 30$ s, but depending on concentration). The resist damage for Na_2S solutions was widespread but concentrated at the pattern edges. We suspect this occurs because Na_2S is a much stronger base than $(NH_4)_2S_x$; UV-exposed photoresist is normally developed in 2.38% TMAH solution, which is also basic. We performed the remainder of the studies in aqueous $(NH_4)_2S_x$, since it was the only passivation solution for which both photo- and EBL-resists remain intact for long immersions.

Appendix B: Initial characterization of passivation solutions and their robustness

Once we had established the suitability of the aqueous $(NH_4)_2S_x$ solutions, we utilized PL measurements on (100) GaAs to confirm their efficacy. The passivated samples used in this section are listed in Table II. Figure 5(a) shows PL intensity versus wavelength for Sample B5 treated with the strong solution and Sample B6 treated with the weak solution, with the PL intensity normalized to the signal obtained from an otherwise equivalent untreated sample. A $\sim 40\times$ and $\sim 90\times$ increase in

TABLE II. List of samples discussed in Appendix B. All are bulk, passivated GaAs wafer pieces used for PL.

Sample	Wafer	Surface	Passivation
B5	bulk	(100)	strong
B6	bulk	(100)	weak
B7	bulk	(100)	strong
B8	bulk	(100)	weak
B9	bulk	(100)	weak + photoprocessed

intensity is observed for Samples B5 and B6 respectively. The 2.25× improvement in PL intensity produced by increasing passivation solution concentration by a factor of approximately 200 is small compared to the 40× increase in PL intensity produced by simply using the weak solution. Regarding the appearance of the treated surfaces, Nannichi *et al.*[35] report deposition of a thin off-white precipitate film on the GaAs surface after $(NH_4)_2S_x$ passivation. We only obtain this when the wafer is removed directly from the strong solution, and it could be prevented by diluting this treatment with H_2O prior to removing the sample. We found no appreciable change in PL intensity when using this dilution method for preventing sulfide film formation.

We also used PL to study the robustness of the treatment over time under different storage conditions. Figure 5(b) shows that the PL intensity for B7 was only 15% lower after being stored for a week in the dark, under room atmosphere conditions, than it was when measured immediately after passivation. This discrepancy is within the experimental error for a PL measurement, suggesting that there has been little to no degradation of the passivation. This confirms that the passivation remains intact during the short exposure to air between passivation and gate deposition for the heterostructure devices D2-D5. In some instances, it is desirable to thermally anneal the sample to ∼ 350°C, however, patterned resists are generally destroyed at such high temperatures. In such cases, passivation and annealing would need be performed prior to resist deposition. With this in mind, we also studied the robustness of a passivated surface to subsequent photolithographic processing. We passivated Samples B8 and B9 together and then processed B9 further by depositing an AZ nLOF2020 resist film, baking the chip at 110°C for 60 s and developing in TMAH. Sample B9 was not exposed to UV light as the surface regions beneath the gates are normally protected by the photomask during pattern exposure for this negative resist. As Fig. 5(c) shows, the PL intensity was not reduced by the addition of photoprocessing steps. This confirms that device D6 should have remained passivated during photoprocessing for gate deposition.

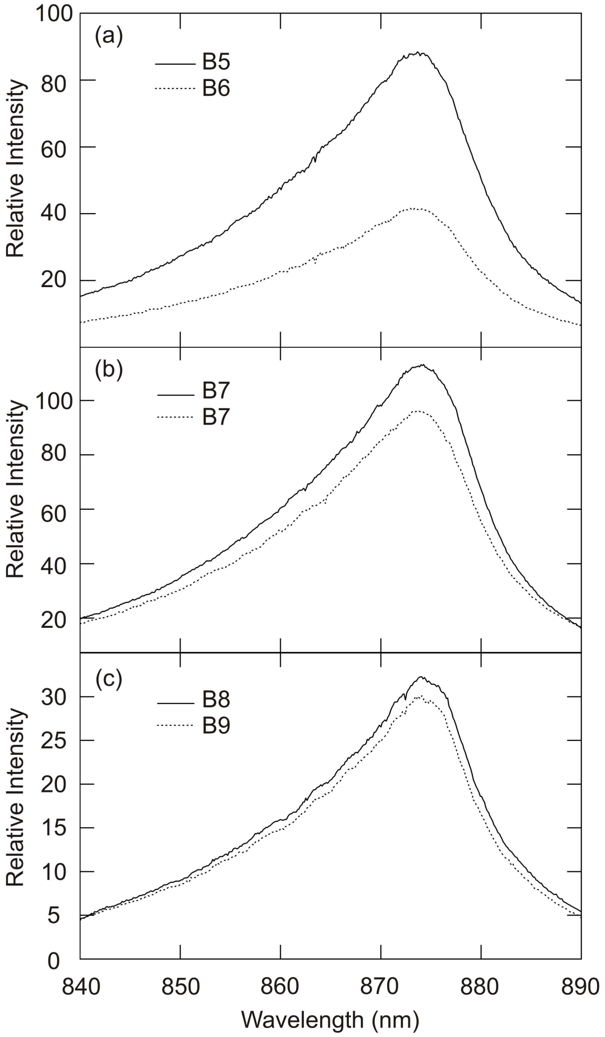

FIG. 5. (a) Photoluminescence (PL) intensity versus luminescence wavelength for Samples B5 and B6. The yields given are normalized to the PL spectrum obtained from an otherwise equivalent, untreated sample. (b) PL spectrum of Sample B7 obtained immediately after passivation (solid line) and after one week (dashed line) of storage in the dark under room atmosphere conditions. (c) PL spectrum of Samples B8 and B9 showing that comparable PL intensities are obtained whether or not the sample is photoprocessed after passivation.

Appendix C: Raw photoluminescence data of unpassivated (100) and (311)A GaAs surfaces

The data presented in Fig. 2(a/b) were normalized to the peak of untreated (100)/(311)A oriented GaAs, respectively. Figure 6 shows the raw, as-recorded intensity for these two reference samples. In contrast to all other presented PL data, the data in Fig. 6 has not been normalized; the intensity here refers to the recorded intensity incident on the CCD camera. Note also that the (100) reference sample used for Fig. 6 is not the same as the references used in Appendix B; each experiment had its own unique reference sample and the data in Fig. 6

is from reference samples used in conjunction with the data in Fig. 2. In each case, the reference and passivated samples were cleaved from positions immediately adjacent to each other on the host wafer to ensure optimum similarity for the two surfaces.

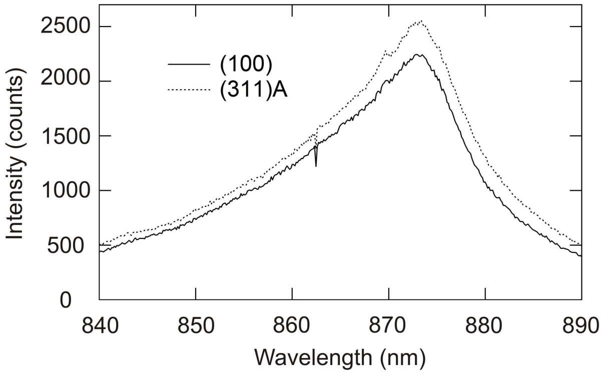

FIG. 6. Photoluminescence intensity versus luminescence wavelength for the two samples used as references in Section IIIB. The intensity used here is the recorded intensity incident on the CCD camera.

---

[*] adam.micolich@nanoelectronics.physics.unsw.edu.au

[1] M.V. Lebedev, Prog. Surf. Sci. **70**, 153 (2002).

[2] D. Liu, T. Zhang, R.A. LaRue, J.S. Harris Jr. and T.W. Sigmon, Appl. Phys. Lett. **53**, 1059 (1988).

[3] C.J. Sandroff, R.N. Nottenburg, J.-C. Bischoff and R. Bhat, Appl. Phys. Lett. **51**, 33 (1987).

[4] E. Yablonovitch, C.J. Sandroff, R. Bhat and T. Gmitter, Appl. Phys. Lett. **51**, 439 (1987).

[5] R.S. Besser and C.R. Helms, Appl. Phys. Lett. **52**, 1707 (1988).

[6] M.S. Carpenter, M.R. Melloch and T.E. Dungan, Appl. Phys. Lett. **53**, 66 (1988).

[7] C.J. Sandroff, M.S. Hegde, L.A. Farrow, C.C. Chang and J.P. Harbison, Appl. Phys. Lett. **54**, 362 (1989).

[8] R. Cohen, L. Kronik, A. Vilan, A. Shanzer and D. Cahen, Adv. Mater. **12**, 33 (2000).

[9] V.N. Bessolov, E.V. Konenkova and M.V. Lebedev, J. Vac. Sci. Technol. B **14**, 2761 (1996).

[10] V.N. Bessolov, E.V. Konenkova and M.V. Lebedev, Mat. Sci. Eng. B **44**, 376 (1997).

[11] V.N. Bessolov, M.V. Lebedev, N. Minh Binh, M. Friedrich and D.R.T. Zahn, Semicond. Sci. Technol. **13**, 611 (1998).

[12] Z.S. Li, W.Z. Cai, R.Z. Su, G.S. Dong, D.M. Huang, X.M. Ding, X.Y. Hou and X. Wang, Appl. Phys. Lett. **64**, 3425 (1994).

[13] V.I. Gaman, V.M. Kalygina and A.V. Panin, Solid State Electron. **43**, 583 (1999).

[14] T. Tiedje, K.M. Colbow, D. Rogers, Z. Fu and W. Eberhardt, J. Vac. Sci. Technol. B **7**, 837 (1989).

[15] S. Conrad, D.R. Mullins, Q.-S. Xin and X.-Y. Zhu, Appl. Surf. Sci. **107**, 145 (1996).

[16] C.I.H. Ashby, K.R. Zavadil, A.J. Howard and B.E. Hammons, Appl. Phys. Lett. **64**, 2388 (1994).

[17] Y. Hanein, U. Meirav, D. Shahar, C.C. Li, D.C. Tsui and H. Shtrikman, Phys. Rev. Lett. **80**, 1288 (1998).

[18] S.J. Papadakis, E.P. De Poortere, H.C. Manoharan, M. Shayegan and R. Winkler, Science **283**, 2056 (1999).

[19] E. Tutuc, M. Shayegan and D.A. Huse, Phys. Rev. Lett. **93**, 036802 (2004).

[20] W.R. Clarke, A.P. Micolich, A.R. Hamilton, M.Y. Simmons, C.B. Hanna, J.R. Rodriguez, M. Pepper and D.A. Ritchie, Phys. Rev. B **71**, 081304 (2005).

[21] R. Winkler, S.J. Papadakis, E.P. De Poortere and M. Shayegan, Phys. Rev. Lett. **85**, 4574 (2000).

[22] R. Danneau, O. Klochan, W.R. Clarke, L.H. Ho, A.P. Micolich, M.Y. Simmons, A.R. Hamilton, M. Pepper, D.A. Ritchie and U. Zülicke, Phys. Rev. Lett. **97**, 026403 (2006).

[23] J.C.H. Chen, O. Klochan, A.P. Micolich, A.R. Hamilton, T.P. Martin, L.H. Ho, U. Zülicke, D. Reuter and A.D. Wieck, New J. Phys. **12**, 033043 (2010).

[24] R. Winkler, E. Tutuc, S.J. Papadakis, S. Melinte, M. Shayegan, D. Wasserman and S.A. Lyon, Phys. Rev. B **72**, 195321 (2005).

[25] R. Danneau, O. Klochan, W.R. Clarke, L.H. Ho, A.P. Micolich, M.Y. Simmons, A.R. Hamilton, M. Pepper and D.A. Ritchie, Phys. Rev. Lett. **100**, 016403 (2008).

[26] A.P. Micolich, J. Phys.: Condens. Matter **23**, 443201 (2011).

[27] J.-B. Yau, E.P. De Poortere and M. Shayegan, Phys. Rev. Lett. **88**, 146801 (2002).

[28] O. Klochan, A.P. Micolich, A.R. Hamilton, K. Trunov, D. Reuter and A.D. Wieck, Phys. Rev. Lett. **107**, 076805 (2011).

[29] D. Heiss, S. Schaeck, H. Huebl, M. Bichler, G. Abstreiter, J.J. Finley, D.V. Bulaev and D. Loss, Phys. Rev. B **76**, 241306 (2007).

[30] B.D. Gerardot, D. Brunner, P.A. Dalgarno, P. Öhberg, S. Seidl, M. Kroner, K. Karrai, N.G. Stolz, P.M. Petroff and R.J. Warburton, Nature **451**, 441 (2008).

[31] A.M. Burke, D.E.J. Waddington, D.J. Carrad, R.W. Lyttleton, H.H. Tan, P.J. Reece, O. Klochan, A.R. Hamilton, A. Rai, D. Reuter, A.D. Wieck and A.P. Micolich, Phys. Rev. B **86**, 165309 (2012).

[32] C.J. Sandroff, M.S. Hegde and C.C. Chang, J. Vac. Sci. Technol. B **7**, 841 (1989).

[33] C.J. Spindt, D. Liu, K. Miyano, P.L. Meissner, T.T. Chiang, T. Kendelewicz, I. Lindau and W.E. Spicer, Appl. Phys. Lett. **55**, 861 (1989).

[34] J.-F. Fan, H. Oigawa and Y. Nannichi, Jpn. J. Appl. Phys. **27**, L2125 (1988).

[35] Y. Nannichi, J.-F. Fan, H. Oigawa and A. Koma, Jpn. J. Appl. Phys. **27**, L2367 (1988).

[36] Y.-H. Jeong, K.-H. Choi, S.-K. Jo and B. Kang, Jpn. J. Appl. Phys. **34**, 1176 (1995).

[37] J.V. Li, S.L. Chuang, E. Aifer and E.M. Jackson, Appl. Phys. Lett. **90**, 223503 (2007).

[38] D.B. Suyatin, C. Thelander, M.T. Björk, I. Maximov and L. Samuelson, Nanotechnology **18**, 105307 (2007).

[39] V. Besselov and M. Lebedev, Semiconductors **32**, 1141 (1998).

[40] R.S. Besser and C.R. Helms, J. Appl. Phys. **65**, 4306 (1989).

[41] V.N. Bessolov, M.V. Lebedev, and D.R.T. Zahn, J. Appl. Phys. **82**, 2640 (1997).

[42] P. Jin, S.H. Pan, Y.G. Li, G.Z. Zhang and Z.G. Wang, Appl. Surf. Sci. **218**, 211 (2003).

[43] D. Shahrjerdi, E. Tutuc and S.K. Banerjee, Appl. Phys. Lett. **91**, 063501 (2007).

[44] W.I. Wang, E.E. Mendez, T.S. Kuan and L. Esaki, Appl. Phys. Lett. **47**, 826 (1985).

[45] H. Sugahara, M. Oshima, H. Oigawa, H. Shigekawa and Y. Nannichi, J. Appl. Phys. **69**, 4349 (1991).

[46] D. Paget, J.E. Bonnet, V.L. Berkovits, P. Chiaradia and J. Avila, Phys. Rev. B **53**, 4604 (1996).

[47] P. Moriarty, B. Murphy, L. Roberts, A.A. Cafolla, G. Hughes, L. Koenders and P. Bailey, Phys. Rev. B **50**, 14237 (1994).

[48] Z.H. Lu, M.J. Graham, X.H. Feng and B.X. Yang, Appl. Phys. Lett. **62**, 2932 (1993).

[49] T. Scimeca, Y. Watanabe, R. Berrigan and M. Oshima, Phys. Rev. B **46**, 10201 (1992).

[50] C.-D. Tsai and C.-T. Lee, J. Appl. Phys. **87**, 4230 (2000).

[51] M. Sakata and H. Ikoma, Jpn J. Appl. Phys. **33**, 3813 (1994).

[52] B.J. Skromme, C.J. Sandroff, E. Yablonovitch and T. Gmitter, Appl. Phys. Lett. **51**, 2022 (1987).

[53] D.J. Chadi, J. Vac. Sci. Technol. B **3**, 1167 (1985).

[54] K. Stiles and A. Kahn, J. Vac. Sci. Technol. B **3**, 1089 (1985).

[55] H. Hirayama, Y. Matsumoto, H. Oigawa and Y. Nannichi, Appl. Phys. Lett. **54**, 2565 (1989).

[56] M.V. Lebedev and M. Aono, J. Appl. Phys. **87**, 289 (2000).

[57] H. Sugahara, M. Oshima, R. Klauser, H. Oigawa and Y. Nannichi, Surf. Sci. **242**, 335 (1991).

[58] D. Paget, A.O. Gusev and V.L. Berkovits, Phys. Rev. B **53**, 4615 (1996).

[59] V.L. Berkovits, V.N. Bessolov, T.N. L'vova, E.B. Novikov, V.I. Safarov, R.V. Khasieva and B.V. Tsarenkov, J. Appl. Phys. **70**, 3707 (1991).

[60] S.V. Ivanov, P.S. Kop'ev and N.N. Ledentsov, J. Cryst. Growth **108**, 661 (1991).

[61] D.J. Chadi, Phys. Rev. B **29**, 785 (1984).

[62] A. Taguchi and K. Shiraishi, Phys. Rev. B **71**, 035349 (2005).

[63] H. Sugahara, M. Oshima, H. Oigawa and Y. Nannichi, J. Vac. Sci. Technol. A **11**, 52 (1993).

[64] M. Sugiyama, S. Maeyama and M. Oshima, Phys. Rev. B **50**, 4905 (1994).

[65] T. Ohno and K. Shiraishi, Phys. Rev. B **42**, 11194 (1990).

[66] M. Sugiyama, S. Maeyama, M. Oshima, H. Oigawa, Y. Nannichi and H. Hashizume, Appl. Phys. Lett. **60**, 3247 (1992).

[67] M. Sugiyama, S. Maeyama and M. Oshima, Phys. Rev. B **48**, 11037 (1993).

[68] B. Murphy, P. Moriarty, L. Roberts, T. Cafolla, G. Hughes, L. Koenders and P. Bailey, Surf. Sci. **317**, 73 (1994).

[69] T. Ohno, Phys. Rev. B **44**, 6306 (1991).

[70] S.-F. Ren and Y.-C. Chang, Phys. Rev. B **41** 7705 (1990).

[71] J.-F. Fan, H. Oigawa and Y. Nannichi, Jpn. J. Appl. Phys. **27**, L1331 (1988).

[72] H. Sik, Y. Feurprier, C. Cardinaud, G. Turban and A. Scavennec, J. Electrochem. Soc. **144**, 2106 (1997).

[73] L.M. Terman, Solid-state Electron. **5**, 285 (1962).

[74] Z.H. Lu, F. Chatenoud, M.M. Dion, M.J. Graham, H.E. Ruda, I. Koutzarov, Q. Liu, C.E.J. Mitchell, I.G. Hill and A.B. McLean, Appl. Phys. Lett. **67**, 670 (1995).

[75] M.C. Traub, J.S. Biteen, B.S. Brunschwig and N.W. Lewis, J. Am. Chem. Soc. **130**, 955 (2008).

[76] C.J. Sandroff, M.S. Hegde, L.A. Farrow, R. Bhat, J.P. Harbison and C.C. Chang, J. Appl. Phys. **67**, 586 (1990).

[77] B.A. Kuruvilla, S.V. Ghaisas, A. Datta, S. Banerjee and S.K. Kulkarni, J. Appl. Phys. **73**, 4384 (1993).

[78] T. Scimeca, Y. Watanabe, F. Maeda, R. Berrigan and M. Oshima, Appl. Phys. Lett. **62**, 1667 (1993).

[79] M.D. Pashley and D. Li, J. Vac. Sci. Technol. A **12**, 1848 (1994).

[80] C.J. Spindt and W.E. Spicer, Appl. Phys. Lett. **55**, 1653 (1989).

[81] S. Belkouch, C. Aktik, H. Xu and E.L. Ameziane, Solid-state Electron. **39**, 507 (1996).

[82] M. Tabib-Azar, S. Kang, A.N. MacInnes, M.B. Power, A.R. Barron, P.P. Jenkins and A.F. Hepp, Appl. Phys. Lett. **63**, 625 (1993).

[83] A.B.M.O. Islam, K. Asai, K.K. Lim, T. Tambo and C. Tatsuyama, Surf. Sci. **416**, 295 (1998).

[84] X.A. Cao, H.T. Hu, Y. Dong, X.M. Ding and X.Y. Hou, J. Appl. Phys. **86**, 6940 (1999).

[85] P.M. Solomon, C.N. Knoedler and S.L. Wright, IEEE Electron Dev. Lett. **5**, 379 (1984).

[86] B.E. Kane, G.R. Facer, A.S. Dzurak, N.E. Lumpkin, R.G. Clark, L.N. Pfeiffer and K.W. West, Appl. Phys. Lett. **72**, 3506 (1998).

[87] W.R. Clarke, A.P. Micolich, A.R. Hamilton, M.Y. Simmons, K. Muraki and Y. Hirayama, J. Appl. Phys. **99**, 023707 (2006).